Spatial distribution of $\delta^{18}O$ in meteoric precipitation

Gabriel J. Bowen Department of Earth Sciences, University of California, Santa Cruz, California 95064, USA
Bruce Wilkinson Department of Geological Sciences, University of Michigan, Ann Arbor, Michigan 48109, USA

ABSTRACT

Proxy data reflecting the oxygen isotope composition of meteoric precipitation ($\delta^{18}O_{ppt}$) are widely used in reconstructions of continental paleoclimate and paleohydrology. However, actual geographic variation in modern water compositions is difficult to estimate from often sparse data. A first step toward understanding the geologic pattern of change in $\delta^{18}O_{ppt}$ is to describe the modern distribution in terms of principal geographic parameters. To this end, we empirically model relationships between ^{18}O in modern precipitation and latitude and altitude. We then identify geographic areas where large-scale vapor transport patterns give rise to significant deviations from model $\delta^{18}O_{ppt}$ compositions based on latitude and altitude. Model value and residual grids are combined to derive a high-resolution global map of $\delta^{18}O_{ppt}$ that can serve as a spatial reference against which proxy data for paleoprecipitation can be compared. Reiteration of the procedure outlined here, for paleo-$\delta^{18}O_{ppt}$ data, may illuminate past changes in the climatic and physiographic parameters controlling the distribution of $\delta^{18}O$ regimes.

Keywords: isotopes, oxygen, paleoclimates, precipitation.

INTRODUCTION

The oxygen isotope composition of meteoric water as recorded in authigenic minerals and biogenic hardparts has been used extensively in studies of ancient continental climate and hydrology. Important records have been derived from ice cores (e.g., Dansgaard et al., 1993; Thompson et al., 1995; Petit et al., 1999), groundwater (e.g., Rozanski, 1985; Dutton, 1995), speleothems (e.g., Schwarcz, 1986; Dorale et al., 1992; Denniston et al., 1999), meteoric calcite cements (e.g., Hays and Grossman, 1991), freshwater mollusks (e.g., Dettman and Lohmann, 1993), fossil enamel (e.g., Bryant et al., 1996; Fricke et al., 1998; Sharp and Cerling, 1998), soil carbonate (e.g., Koch et al., 1995; Amundson et al., 1996; Cerling and Wang, 1996), iron-oxide minerals (e.g., Bao et al., 1998, 1999), and authigenic clays (e.g., Chamberlain et al., 1999; Chamberlain and Poage, 2000). These records are frequently used to estimate paleotemperature based on the strong spatial correlation between modern $\delta^{18}O_{ppt}$ and local mean annual temperature (Dansgaard, 1964).

It has become increasingly apparent that past changes in atmospheric circulation and other climatic parameters may render simple temperature-based interpretation of paleo-$\delta^{18}O_{ppt}$ data incorrect (Amundson et al., 1996; Edwards et al., 1996; Boyle, 1997; Fricke and O'Neil, 1999; Pierrehumbert, 1999). Theoretical models for $\delta^{18}O_{ppt}$, combining Rayleigh distillation with a more or less comprehensive treatment of the meteorological evolution of individual air parcels, have been developed and applied to individual precipitation events (Covey and Haagenson, 1984) and locations (Dansgaard, 1954; Boyle, 1997; Pierrehumbert, 1999). Similar treatments, coupled to global circulation models (GCMs), have produced reasonably accurate, low-resolution model $\delta^{18}O_{ppt}$ maps for the modern Earth and estimated values for the Last Glacial Maximum (Joussaume et al., 1984; Jouzel et al., 1994; Hoffmann and Heimann, 1997). Application of theoretical models to paleo-$\delta^{18}O_{ppt}$ proxy data, however, is limited by inadequate knowledge of relevant meteorological parameters and uncertainties regarding GCM reproduction of past climates.

Despite the abundance of work that has addressed relationships between climate variables and $\delta^{18}O_{ppt}$, relatively little research has focused on the geographic distribution of $\delta^{18}O_{ppt}$ and its variation through time. To address these issues, a modern spatial reference framework is needed against which ancient values can be compared. Here we develop the necessary framework as a high-resolution map of $\delta^{18}O_{ppt}$ based on an empirically derived model incorporating basic geographic parameters.

DATA

Our effort begins with data from the third release of the International Atomic Energy Agency–World Meteorological Organization Global Network for Isotopes in Precipitation (GNIP) database (IAEA/WMO, 1998). The database includes data from 583 stations, although fewer than half of these have oxygen isotope records representing one or more years (see Rozanski et al., 1993, for a complete review of an earlier release of this data set). Model equations were derived from station geographic data and from average amount-weighted annual $\delta^{18}O_{ppt}$ values that were calculated from the month-by-month GNIP isotopic and precipitation measurements. To calculate annual averages, amount-weighted mean values were calculated for each month for all years represented at each station. These monthly $\delta^{18}O_{ppt}$ values were used to derive an amount-weighted mean annual $\delta^{18}O_{ppt}$ for each of 232 stations. Other routines for calculating average annual $\delta^{18}O_{ppt}$ were explored and do not produce results significantly different from those presented here. The high-resolution map of $\delta^{18}O_{ppt}$ was created by using topographic data from the U.S. Geological Survey ETOPO5 digital elevation model (DEM), with 5 min latitudinal and longitudinal resolution (U.S. National Geophysical Data Center, 1998).

APPROACH

Previously, estimation of $\delta^{18}O_{ppt}$ at a given geographic location has been accomplished by interpolation between GNIP stations or by reference to the nearest station. However, the oxygen isotope composition of precipitation is controlled by Rayleigh distillation of atmospheric vapor, driven primarily by changes in air-mass temperature (e.g., Yurtsever, 1975; Rozanski et al., 1993), and interpolated estimates ignore the geographic parameters that control temperature (latitude and altitude). We incorporate these variables by using the global mean relationships between latitude and altitude and $\delta^{18}O_{ppt}$ to predict local $\delta^{18}O_{ppt}$. Large-scale patterns of atmospheric vapor transport also affect $\delta^{18}O_{ppt}$ by changing the length and origin of vapor-transport pathways (Amundson et al., 1996; Edwards et al., 1996; Boyle, 1997). These effects appear as regional deviations of GNIP station observations from the predictions based on latitude and altitude. We incorporate vapor-transport effects in our best estimate $\delta^{18}O_{ppt}$ map by spatially interpolating the residuals from our altitude and latitude model and adding those to the map grid generated from the model.

MODEL DERIVATION

We used a two-step regression technique to deconvolve the effects of latitude and altitude on $\delta^{18}O_{ppt}$. The negative correlation between $\delta^{18}O_{ppt}$ and the absolute value of station latitude ($|LAT|$, Fig. 1) results from the cooling and distillation of water vapor during transport from low-latitude regions toward the poles. Data from stations at <200 m elevation ($n = 155$) were isolated to evaluate latitudinal variation in $\delta^{18}O_{ppt}$ values while minimizing the complicating effects of topography. The relationship between low altitude station $|LAT|$ (independent variable) and $\delta^{18}O_{ppt}$ (dependent variable) is best described by the second-order polynomial:

$$\delta^{18}O_{ppt} = -0.0051(|LAT|)^2 + 0.1805(|LAT|) - 5.247 \quad (1)$$

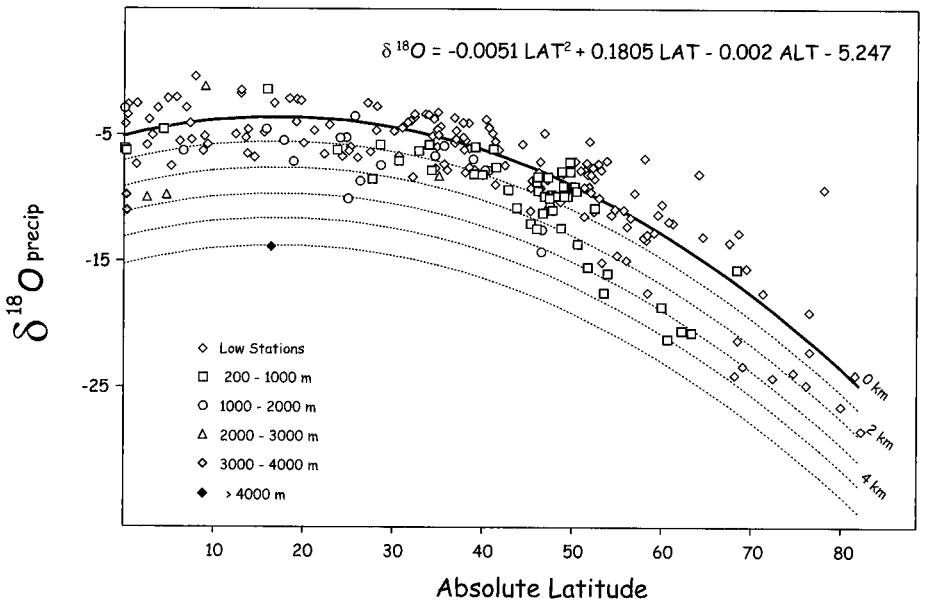

Figure 1. $\delta^{18}O$ of meteoric precipitation plotted against station latitude for 232 GNIP stations, with best-fit polynomial for low-altitude stations (<200 m; solid) and model lines for 1–5 km elevations. Model equation is shown.

(solid line, Fig. 1) for which $r^2 = 0.80$. The shape of this trend is largely the result of the nonlinear relationship between latitude and temperature and is exaggerated by the negative correlation between annual precipitation amount and $\delta^{18}O_{ppt}$ in the tropics (e.g., Rozanski et al., 1993).

There is a tendency for the $\delta^{18}O_{ppt}$ values of stations above 200 m to be below the low-altitude station trend (Fig. 1), and deviations of measured values from the low-altitude trend systematically increase with increasing station altitude (ALT, meters). The association between these parameters is a function of the cooling of air masses as they rise to higher elevations and is roughly linear. To derive the relationship between altitude and $\delta^{18}O_{ppt}$, we first used equation 1 to estimate $\delta^{18}O_{ppt}$ values for all stations based on their latitudes. The negative correlation between $\delta^{18}O_{ppt}$ and altitude (oxygen isotope lapse rate, OILR) was quantified by least-squares regression between station altitudes (independent variable) and the residuals from equation 1 (DEV, dependent variable), where the Y-intercept was fixed at 0. This approach allowed us to examine the latitude-independent effects of altitude on $\delta^{18}O_{ppt}$. The best-fit equation is

$$\mathrm{DEV} = -0.002(\mathrm{ALT}), \quad (2)$$

where $r^2 = 0.17$. This yields an oxygen isotope lapse rate of 2‰/km, a value almost identical to that calculated by Chamberlain and Poage (2000). The slope of this relationship has a standard error of ±0.0002 and is highly significant at the 95% confidence level ($p < 0.0001$).

Our model equation, describing $\delta^{18}O_{ppt}$ for the continents as a function of latitude and altitude, is the sum of equations 1 and 2:

$$\delta^{18}O_{ppt} = -0.0051(|\mathrm{LAT}|)^2 + 0.1805(|\mathrm{LAT}|) - 0.002(\mathrm{ALT}) - 5.247. \quad (3)$$

This formulation assumes that the oxygen isotope lapse rate is similar at all geographic locations, a necessary simplification given the current lack of data from high altitudes. The average difference between $\delta^{18}O_{ppt}$ values estimated from equation 3 and the measured values is −0.21‰ ($\sigma = 2.49$‰). The relationship between estimated and measured values is linear with a slope of 1.04 and $R^2 = 0.76$.

SPATIAL DISTRIBUTION OF MODEL RESIDUALS

Equation 3 was applied to each GNIP station, and a second set of residuals was calculated that describes the difference between observed values and those predicted by the combined model. To investigate the spatial distribution of these residuals, a 0.5° × 0.5° grid was interpolated on a spherical surface. Residuals were weighted according to:

$$\mathrm{weight} = e^{(-d^2/4^\circ)}, \quad (4)$$

where d is the angular distance between a grid point and data point. This function allows relatively smooth interpolation of unevenly spaced data and highlights variation over distances of 10^2 to 10^3 km, a scale at which the effects of large-scale vapor-transport patterns should be evident.

The spatial distribution of interpolated residuals (Fig. 2) shows significant variation at the 10^2 to 10^3 km scale. Low-magnitude interpolated residuals cannot be considered meaningful across regions with sparse data (e.g., Africa and Siberia). In other regions (e.g., South America, southern North America, the Mediterranean, and eastern Europe), however, low-magnitude residuals are interpolated from abundant data and confirm that $\delta^{18}O_{ppt}$ is primarily dependent on latitudinal and altitudinal temperature variations. In addition, there are large oceanic areas (e.g., the northern Atlantic and the western Pacific) where the model is in good agreement with observations made at numerous, but widely separated, island stations.

Regions of high-magnitude residuals occur at northern middle to high latitudes and likely reflect the zonal heterogeneity of vapor transport. In particular, the latitude and altitude model significantly overestimates the $\delta^{18}O$ of precipitation over Canada, while underestimating $\delta^{18}O_{ppt}$ in the Norwegian and Barents Seas. Comparison of the residual map with vertically averaged patterns of vapor transport (Peixoto and Oort, 1992) suggests that residuals in the North Atlantic may relate to northward and eastward transport of moisture across the warm North Atlantic, a process that would provide relatively ^{18}O enriched water to northern coastal Europe. Conversely, overestimation of $\delta^{18}O_{ppt}$ in Canada may be associated with a component of ^{18}O-depleted, Arctic-derived moisture and with eastward transport of moisture across the cool Pacific eastern boundary currents before reaching the continent.

In some cases, adequate explanation of the residuals will require additional data. The anomaly across East Africa, for example, reflects the fact that water compositions from two high-altitude stations (Addis Ababa at 2.36 km and Entebbe at 1.16 km) are close to those anticipated for sea-level stations at that latitude. Recently published $\delta^{18}O_{ppt}$ measurements from a transect (10–4050 m altitude, $n = 20$) in equatorial East Africa (Gonfiantini et al., 2001) are heavier than the values predicted by equation 3 according to:

$$\delta^{18}O_{measured} - \delta^{18}O_{model} = 0.0004(\mathrm{ALT}) + 1.371, \quad (5)$$

where the $r^2 = 0.57$ and the slope is significant at 95% confidence with $p < 0.001$. This suggests that the oxygen isotope lapse rate in this region is 20% lower than the global average and, although the East African anomaly may characterize precipitation at all altitudes,

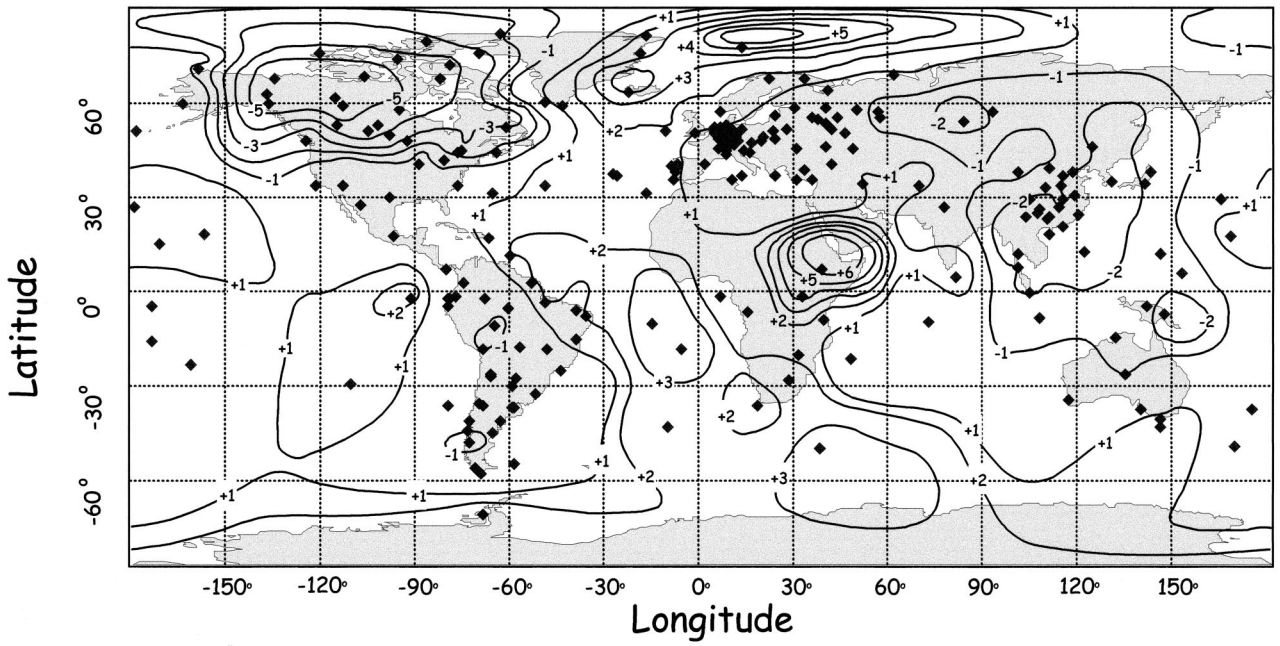

Figure 2. GNIP stations (shaded diamonds) with model residuals contoured at 1‰ intervals. Note significant residual values over East Africa and at high latitudes over northern North America and North Atlantic.

its magnitude in Figure 2 is exaggerated because data from this region are from high-altitude stations.

SPATIAL DISTRIBUTION OF $\delta^{18}O$ IN METEORIC PRECIPITATION

A 5′ × 5′ grid of equation 3 residuals was interpolated from the 0.5° × 0.5° grid just discussed. This grid was added to a 5′ × 5′ grid generated from application of equation 3 to the ETOPO5 DEM grid points, producing a map grid representing our best estimation of $\delta^{18}O_{ppt}$ (Fig. 3). The pattern of $\delta^{18}O_{ppt}$ distribution is similar to that previously documented (Yurtsever, 1975), but with considerable refinement. The map reproduces the $\delta^{18}O_{ppt}$ of continental GNIP stations closely, with an average error of 0.08‰ (σ = 0.85‰, n = 168). The relationship between map $\delta^{18}O_{ppt}$ values and measurements is linear with a slope of 1.00 and R^2 = 0.97. To test the predictive power of the map, we compared $\delta^{18}O_{ppt}$ data from Goldstone, California (35.35°N, 116.89°W, 920 m; Friedman et al., 1992), and Ames, Iowa (42.03°N, 93.68°W, 287 m; Simpkins, 1995), to Figure 3 values and to estimates from linear interpolation between the

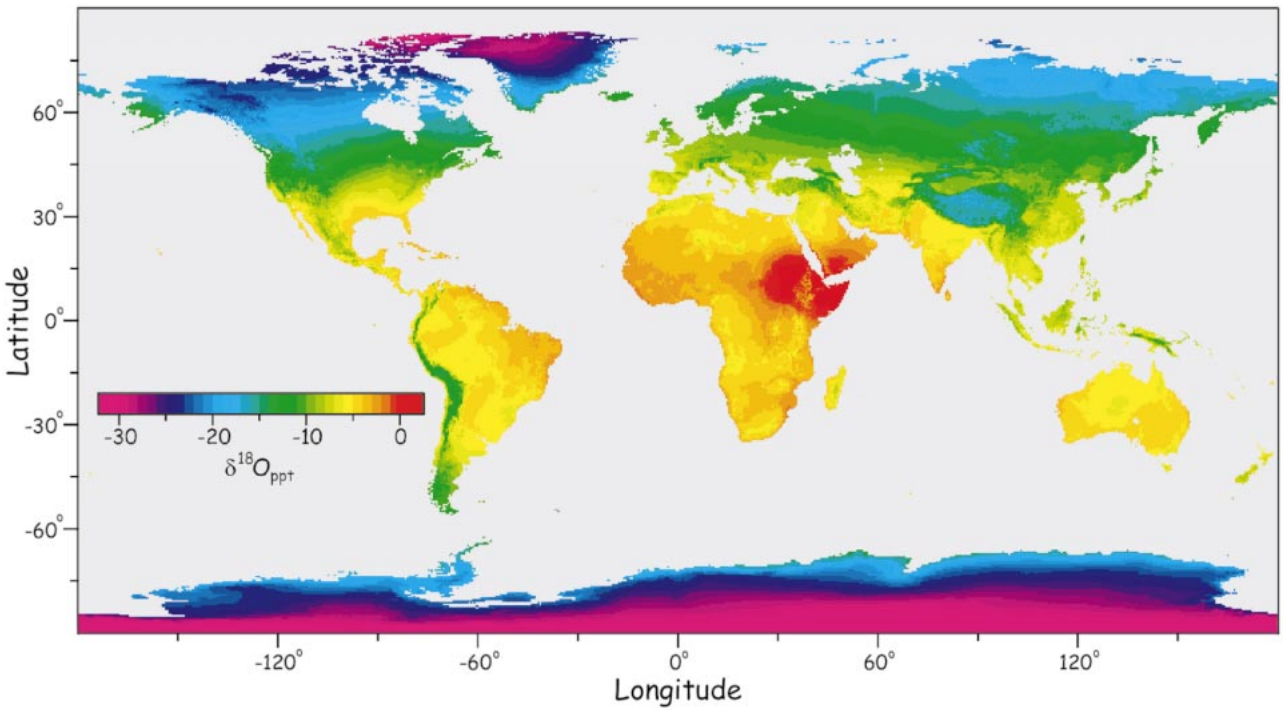

Figure 3. Map of $\delta^{18}O_{ppt}$ calculated for continents at 5′ × 5′ geographic resolution. Map values are sum of model-derived $\delta^{18}O_{ppt}$ estimates from latitude and altitude data (Fig. 1) and spatially interpolated model residuals (Fig. 2). Color bands represent 1‰ intervals between −30‰ and 0‰.

nearest GNIP stations. Map and linearly interpolated estimated values at Goldstone were −7.6‰ and −7.1‰, respectively, compared to the measured value of −10.4‰. At Ames, map and interpolated predictions were −8.9‰ and −9.9‰, respectively, and the measured value was −8.0‰. In each case, the map values more closely approximate measurements. The estimation of confidence limits for map predictions will be the focus of future work.

The map shown as Figure 3 affords several potential uses. Because the map accounts for the effect of local topography on $\delta^{18}O_{ppt}$, temporal change in $\delta^{18}O_{ppt}$ at a single location may be better evaluated with reference to map values than interpolated estimates. Second, the map depicts modern, globally averaged relationships between $\delta^{18}O_{ppt}$ and a number of explicit (latitude, altitude) and more obscure (vapor sources, storm tracks) geographic variables. Reiteration of the process described here for high-quality paleo-$\delta^{18}O_{ppt}$ proxy data representing a previous climate state will be a first step toward understanding the stability of these relationships through time. Finally, because regions where $\delta^{18}O_{ppt}$ deviates significantly from the global mean geographic and physiographic trends may reflect large-scale vapor-transport patterns, recognition of such areas in a data set for paleo-$\delta^{18}O_{ppt}$ could highlight temporal variations in atmospheric or oceanic circulation.

ACKNOWLEDGMENTS

We thank the University of California, Santa Cruz, paleoclimate modeling group and Justin Revenaugh for assistance with data processing and display. Early drafts of the manuscript benefited from reviews by C. Page Chamberlain, Andrea Dutton, David Fox, Linda Ivany, Paul Koch, and Michal Kowalewski. Bowen was supported by the National Science Foundation Graduate Research Fellowship Program.

REFERENCES CITED

Amundson, R.G., Chadwick, O.A., Kendall, C., Wang, Y., and DeNiro, M.J., 1996, Isotopic evidence for shifts in atmospheric circulation patterns during the late Quaternary in mid-North America: Geology, v. 24, p. 23–26.

Bao, H., Koch, P.L., and Hepple, R.P., 1998, Hematite and calcite coatings on fossil vertebrates: Journal of Sedimentary Research, v. 68, p. 727–738.

Bao, H., Koch, P.L., and Rumble, D., III, 1999, Paleocene-Eocene climatic variation in western North America; evidence from the $\delta^{18}O$ of pedogenic hematite: Geological Society of America Bulletin, v. 111, p. 1405–1415.

Boyle, E.A., 1997, Cool tropical temperatures shift the global $\delta^{18}O$-*T* relationship: An explanation for the ice core $\delta^{18}O$-borehole thermometry conflict?: Geophysical Research Letters, v. 24, p. 273–276.

Bryant, J.D., Koch, P.L., Froelich, P.N., Showers, W.J., and Genna, B.J., 1996, Oxygen isotope partitioning between phosphate and carbonate in mammalian apatite: Geochimica et Cosmochimica Acta, v. 60, p. 5145–5148.

Cerling, T.E., and Wang, Y., 1996, Stable carbon and oxygen isotopes in soil CO_2 and soil carbonate: Theory, practice, and application to some prairie soils of upper midwestern North America, *in* Boutton, T.W., and Yamasaki, S., eds., Mass spectrometry of soils: New York, Marcel Dekker, Inc., p. 217–231.

Chamberlain, C.P., and Poage, M.A., 2000, Reconstructing the paleotopography of mountain belts from the isotopic composition of authigenic minerals: Geology, v. 28, p. 115–118.

Chamberlain, C.P., Poage, M.A., Craw, D., and Reynolds, R.C., 1999, Topographic development of the Southern Alps recorded by the isotopic composition of authigenic clay minerals, South Island, New Zealand: Chemical Geology, v. 155, p. 279–294.

Covey, C., and Haagenson, P.L., 1984, A model of oxygen isotope composition of precipitation: Implications for paleoclimate data: Journal of Geophysical Research, v. 89, p. 4647–4655.

Dansgaard, W., 1954, The O^{18}-abundance in fresh water: Geochimica et Cosmochimica Acta, v. 6, p. 241–260.

Dansgaard, W., 1964, Stable isotopes in precipitation: Tellus, v. 16, p. 436–468.

Dansgaard, W., Johnsen, S.J., Clausen, H.B., Dahl-Jensen, D., Gundestrup, N.S., Hammer, C.U., Hvidberg, C.S., Steffensen, J.P., Sveinbjornsdottir, A.E., Jouzel, J., and Bond, G., 1993, Evidence for general instability of past climate from a 250-kyr ice-core record: Nature, v. 364, p. 218–220.

Denniston, R.F., Gonzalez, L.A., Asmerom, Y., Baker, R.G., Reagan, M.K., and Bettis, E.A., III, 1999, Evidence for increased cool season moisture during the middle Holocene: Geology, v. 27, p. 815–818.

Dettman, D.L., and Lohmann, K.C, 1993, Seasonal change in Paleogene surface water $\delta^{18}O$; fresh-water bivalves of western North America, *in* Swart, P.K., et al., eds., Climate change in continental isotopic records: American Geophysical Union Geophysical Monograph 78, p. 153–164.

Dorale, J.A., Gonzalez, L.A., Reagan, M.K., Pickett, D.A., Murrell, M.T., and Baker, R.G., 1992, A high-resolution record of Holocene climate change in speleothem calcite from Cold Water Cave, northeast Iowa: Science, v. 258, p. 1626–1630.

Dutton, A.R., 1995, Groundwater isotopic evidence for paleorecharge in U.S. High Plains aquifers: Quaternary Research, v. 43, p. 221–231.

Edwards, T.W.D., Wolfe, B.B., and MacDonald, G.M., 1996, Influence of changing atmospheric circulation on precipitation $\delta^{18}O$-temperature relations in Canada during the Holocene: Quaternary Research, v. 46, p. 211–218.

Fricke, H.C., and O'Neil, J.R., 1999, The correlation between $^{18}O/^{16}O$ ratios of meteoric water and surface temperature: Its use in investigating terrestrial climate change over geologic time: Earth and Planetary Science Letters, v. 170, p. 181–196.

Fricke, H.C., Clyde, W.C., and O'Neil, J.R., 1998, Intratooth variations in $\delta^{18}O$ (PO_4) of mammalian tooth enamel as a record of seasonal variations in continental climate variables: Geochimica et Cosmochimica Acta, v. 62, p. 1839–1850.

Friedman, I., Smith, G.I., Gleason, J.D., Warden, A., and Harris, J.M., 1992, Stable isotope composition of waters in southeastern California: 1. Modern precipitation: Journal of Geophysical Research, v. 97, p. 5795–5812.

Gonfiantini, R., Roche, M.A., Olivry, J.C., Fontes, J.C., and Zuppi, G.M., 2001, The altitude effect on the isotopic composition of tropical rains: Chemical Geology, v. 181, p. 147–167.

Hays, P.D., and Grossman, E.L., 1991, Oxygen isotopes in meteoric calcite cements as indicators of continental paleoclimate: Geology, v. 19, p. 441–444.

Hoffmann, G., and Heimann, M., 1997, Water isotope modeling in the Asian monsoon region: Quaternary International, v. 37, p. 115–128.

IAEA/WMO, 1998, Global network for isotopes in precipitation. The GNIP database. Release 3, October 1999: URL: http://www.iaea.org/programs/ri/gnip/gnipmain.htm (11/2000).

Joussaume, S., Sadourny, R., and Jouzel, J., 1984, A general circulation model of water isotope cycles in the atmosphere: Nature, v. 311, p. 24–29.

Jouzel, J., Koster, R.D., Suozzo, R.J., and Russell, G.L., 1994, Stable water isotope behavior during the Last Glacial Maximum: A general circulation model analysis: Journal of Geophysical Research, v. 99, p. 25 791–25 801.

Koch, P.L., Zachos, J.C., and Dettman, D.L., 1995, Stable isotope stratigraphy and paleoclimatology of the Paleogene Bighorn Basin (Wyoming, USA): Palaeogeography, Palaeoclimatology, Palaeoecology, v. 115, p. 61–89.

Peixoto, J.P., and Oort, A.H., 1992, Physics of climate: New York, American Institute of Physics, 520 p.

Petit, J.R., Jouzel, J., Raynaud, D., Barkov, N.I., Barnola, J.M., Basile, I., Bender, M., Chappellaz, J., Davis, M., Delaygue, G., Delmotte, M., Kotlyakov, V.M., Legrand, M., Lipenkov, V.Y., Lorius, C., Pepin, L., Ritz, C., Saltzmann, E., and Stievenard, M., 1999, Climate and atmospheric history of the past 420 000 years from the Vostok ice core, Antarctica: Nature, v. 399, p. 429–436.

Pierrehumbert, R.T., 1999, Huascaran $\delta^{18}O$ as an indicator of tropical climate during the Last Glacial Maximum: Geophysical Research Letters, v. 26, p. 1345–1348.

Rozanski, K., 1985, Deuterium and oxygen-18 in European groundwaters; links to atmospheric circulation in the past: Chemical Geology, v. 52, p. 349–363.

Rozanski, K., Araguas-Araguas, L., and Gonfiantini, R., 1993, Isotopic patterns in modern global precipitation, *in* Swart, P.K., et al., eds., Climate change in continental isotopic records: American Geophysical Union Geophysical Monograph 78, p. 1–36.

Schwarcz, H.P., 1986, Geochronology and isotopic geochemistry of speleothems, *in* Fritz, P., and Fontes, J.C., eds., Handbook of environmental isotope geochemistry: Amsterdam, Elsevier, p. 271–304.

Sharp, Z.D., and Cerling, T.E., 1998, Fossil isotope records of seasonal climate and ecology—Straight from the horse's mouth: Geology, v. 26, p. 219–222.

Simpkins, W.W., 1995, Isotopic composition of precipitation in central Iowa: Journal of Hydrology, v. 172, p. 185–207.

Thompson, L.G., Mosley-Thompson, E., Davis, M.E., Lin, P.N., Henderson, K.A., Cole-Dai, J., Bolzan, J.F., and Liu, K.B., 1995, Late glacial stage and Holocene tropical ice core records from Huscaran, Peru: Science, v. 269, p. 46–50.

U.S. National Geophysical Data Center (NGDC), 1998, ETOPO-5 five minute gridded world elevation: Boulder, Colorado, USA, NGDC, URL: http://www.grid.unep.ch/datasets/earth.html (11/2000).

Yurtsever, Y., 1975, Worldwide survey of stable isotopes in precipitation: Vienna, International Atomic Energy Agency, Report of the Isotope Hydrology Section, 40 p.

Manuscript received September 20, 2001
Revised manuscript received December 5, 2001
Manuscript accepted December 6, 2001

Printed in USA